DEPARTMENT OF THE INTERIOR
U.S. GEOLOGICAL SURVEY

In Situ Geomechanics of Crystalline and Sedimentary Rocks

Part VIII: Anisotropic Characterization of Pierre Shale--Preliminary Results

By

Henri S. Swolfs[1] and Thomas C. Nichols, Jr.[1]

Open-File Report 87-417

1987

[1]U.S. Geological Survey
Denver, Colorado

CONTENTS

IN SITU GEOMECHANICS OF CRYSTALLINE AND SEDIMENTARY ROCKS

PART VIII: ANISOTROPIC CHARACTERIZATION OF PIERRE SHALE--PRELIMINARY RESULTS

By Henri S. Swolfs and Thomas C. Nichols, Jr.

PREFACE

This report is the eighth of a series summarizing the results of the U.S. Geological Survey's research program in geomechanics aimed at investigating and assessing the potential of crystalline and sedimentary rock masses as geological repositories of nuclear waste. The first seven parts of this series of reports are referenced below:

Savage, W.Z., and Swolfs, H.S., 1980, The long-term deformation and time-temperature correspondence of viscoelastic rock--an alternative theoretical approach, Pt. 1 of In situ geomechanics of crystalline and sedimentary rocks: U.S. Geological Survey Open-File Report 80-708, 21 p.

Smith, W.K., 1982, Two BASIC computer programs for the determination of in sity stresses using the CSIRO hollow inclusion stress cell and the USBM borehole deformation gage [Pt. 2 of In situ geomechanics of crystalline and sedimentary rocks]: U.S. Geological Survey Open-File Report 82-489, 40 p.

Swolfs, H.S., 1982, First experiences with the C.S.I.R.O. hollow-inclusion stress cell, Pt. 3 of In situ geomechanics of crystalline and sedimentary rocks: U.S.Geological Survey Open-File Report 82-990, 10 p.

Nichols, T.C., Jr., 1983, Continued field testing of the modified U.S. Geological Survey 3-D borehole stress probe, Pt. 4 of In situ geomechanics of crystalline and sedimentary rocks: U.S. Geological Survey Open-File Report 83-750, 11 p.

Savage, W.Z., Powers, P.S., and Swolfs, H.S., 1984, RVT--A FORTRAN program for an exact elastic solution for tectonic and gravity stresses in isolated symmetric ridges and alleys, Pt. 5 of In situ geomechanics of crystalline and sedimentary rocks: U.S. Geological Survey Open-File Report 84-827, 12 p.

Swolfs, H.S., and Powers, P.S., 1985, An update on two BASIC computer programs for the determination of in situ stresses using the CSIRO hollow inclusion cell and the USBM borehole deformation gage, Pt. 6 of In situ geomechanics of crystalline and sedimentary rocks: U.S. GeologicalSurvey Open-File Report 85-509, 15 p.

Savage, W.Z., and Swolfs, H.S., 1987, SLIP--A FORTRAN computer program for computing the potential for sliding on arbitrarily oriented weakness planes in triaxial stress states, Pt. 7 of In situ geomechanics of crystalline and sedimentary rocks: U.S. Geological Survey Open-File Report 87-82, 18 p.

Published journal articles that report on the findings of this program are references below:

Swolfs, H.S., and Kibler, J.S., 1982, A note on the Goodman Jack: Rock Mechanics, v. 15, no. 2, p. 57-66.

Swolfs, H.S., 1983, Aspects of the size-strength relationship of unjointed rocks: Chapter 51 in Rock Mechanics--Theory-Experiment-Practice: 24th U.S. Symposium on Rock Mechanics, College Station, Texas, p. 501-510.

Swolfs, H.S., 1984, The triangular stress diagram - a graphical representation of crustal stress measurements: U.S. Geological Survey Professional Paper 1291, 19 p.

Swolfs, H.S., and Savage, W.Z., 1984, Site characterization studies of a volcanic cap rock, Chapter 39 in Rock Mechanics in Productivity and Protection: 25th U.S. Symposium on Rock Mechanics, Evanston, Illinois, p. 370-380.

Savage, W.Z., Swolfs, H.S., and Powers, P.S., 1985, Gravitational stresses in long symmetric ridges and valleys: International Journal of Rock Mechanics, Mining Sciences, and Geomechanical Abstracts, v. 22, no. 5, p. 291-302.

Swolfs, H.S., and Savage, W.Z., 1985, Topography, stresses, and stability at Yucca Mountain, Nevada, in Research & Engineering Applications in Rock Masses: 26th U.S. Symposium on Rock Mechanics, v. 2, p. 1121-1129.

Savage, W.Z., and Swolfs, H.S., 1986, Tectonic and gravitational stress in long symmetric ridges and valleys: Journal of Geophysical Research, v. 91, no. B3, p. 3677-3685.

Swolfs, H.S., and Savage, W.Z., 1986, Topographic modification of in situ stress in extensional and compressional tectonic environments: Proceedings of the International Symposium on Rock Stress and Rock Stress Measurements, Stockholm, Sweden, p. 89-98.

Swolfs, H.S., and Savage, W.Z., 1987, Analysis of slip potential in faulted rocks: Geological Society of America Abstracts with Programs, Rocky Mountain Section, v. 19, no. 5, p. 338.

Part VIII: Anisotropic Characterization of Pierre Shale--Preliminary Results

By

Henri S. Swolfs and Thomas C. Nichols, Jr.

ABSTRACT

True triaxial compression tests, performed on a 10-cm (4-in.) cubical specimen of Pierre Shale, show that this thinly bedded rock is highly anisotropic. The Young's moduli, E_x and E_y, measured in two orthogonal directions parallel to bedding are about three times greater than E_z measured normal to bedding. Poisson's ratios measured in directions parallel to bedding (ν_{xy}, ν_{yx}, ν_{zx}, and ν_{zy}) vary between 0.20 and 0.40 when loads are applied along directions parallel and normal to bedding. When loads are applied parallel to bedding the Poisson's ratios measured normal to bedding (ν_{xz} and ν_{yz}) approach a value of 1.0. This sample of Pierre Shale may be described as elastically orthotropic with a tendency toward transverse isotropy coincident with the principal material directions. Using the highly directional deformation properties of the shale, the gravity-induced stresses at shallow crustal depths are calculated to show that the horizontal stresses (σ_x and σ_y) in this anisotropic material are greater than the vertical stress component ($\sigma_z = \rho gh$).

INTRODUCTION

In the Earth's crust, geologic materials are subjected to three-dimensional states of stress (Swolfs, 1984). Thus for realistic simulation of the field conditions and development of constitutive models, it is appropriate to test rock specimens under truly triaxial states of stress. Multiaxial testing has been done to determine the shearing strength and faulting behavior of intact rocks (Mogi, 1971; Reches and Dieterich, 1983), the failure strength of jointed model materials (Reik and Zacas, 1978) and schistose rocks (Akai and others, 1970), and the constitutive behavior of coals (Ko and Gerstle, 1976).

This report presents the results of two experiments conducted on a cubical specimen of Pierre Shale using a multiaxial testing apparatus at the University of Colorado. The experiments were designed to investigate the feasibility of determining the deformational properties of stiff, moisture-sensitive clay shales under confining pressures of up to 10 megapascals (MPa).

MATERIAL AND SITE DESCRIPTION

The sample used for these experiments was a 10-cm (4-in.) cube of horizontally bedded Pierre Shale. The bedding consisted of thin layers of dark grey mudstone with occasional fine layers of calcareous silt particles. The mudstone was dominantly a silty clay containing a large amount of mixed-layer smectites (swelling clays).

The sample was taken from an unoriented 18-cm- (7.1-in.) diameter core obtained at the Norden dam site, O'Neill Unit, located on the Niobrara River, 27 km (16.7 mi) northwest of Ainsworth, Nebraska. The core hole, situated in the SE corner of Section 34, T. 33 N., R.23 W. was drilled in December 1979. The core recovered from the drill hole was immediately wrapped in heavy gauge aluminum foil, coated with wax, sealed in 20-cm- (7.9-in.) diameter plastic pipe, and transported by truck to the U.S. Geological Survey laboratories in Denver, Colorado.

SAMPLE PREPARATION PROCEDURES

The core selected for triaxial testing was taken from a depth of 92 m (302 ft). It was chosen because of its uniform texture and lack of incipient fractures. To prepare the sample for testing, a piece of the 18-cm- (7.1-in.) diameter core was trimmed to a 10-cm (4-in.) cube by making six orthogonal cuts with a large rock saw blade. A mixture of water and water-soluble oil was used as a cutting fluid. The sample was wrapped with aluminum foil and waxed after each cut to avoid contamination and disintegration. By properly aligning the sample with respect to bedding during the trimming procedure, a suitable cube was obtained for testing.

EXPERIMENTAL PROCEDURES AND RESULTS

Equipment

The multiaxial testing apparatus, a novel piece of laboratory equipment, provides a means of testing rocks under uniaxial, biaxial, or triaxial compressive loads (e.g., Desai and others, 1982). It is designed to allow independent application of three principal stresses to achieve any stress path in principal stress space. With a capacity of 69 MPa (10,000 psi), the apparatus can be used to test cubical samples 102 mm (4 in.) on a side.

The device consists of a rigid steel frame with six aluminum detachable walls. Three pairs of hydraulically pressured fluid bags or cushions are used to apply compressive loads to the sides of the cubical sample and three hand pumps provide hydraulic pressure. The flexible latex cushions are mounted on the walls that are, in turn, bolted to the massive test frame. An expanded view of one of the six loading systems is shown in figure 1. Using flexible cushions, rather than rigid steel platens, to apply loads results in uniform and known boundary stresses across all six faces of the cubical sample. End effects that are commonly associated with standard triaxial testing apparatus are, therefore, reduced to a minimum. The surface deformations of the six faces of the test sample are measured in each of the three principal directions by a set of three proximity transducers mounted on each wall behind the fluid cushions. These transducers measure the relative distance between a conductive brass target on the faces of the test sample and a coil embedded in the transducer tip. Both normal and shear strains can be determined as loading takes place (Desai and others, 1982).

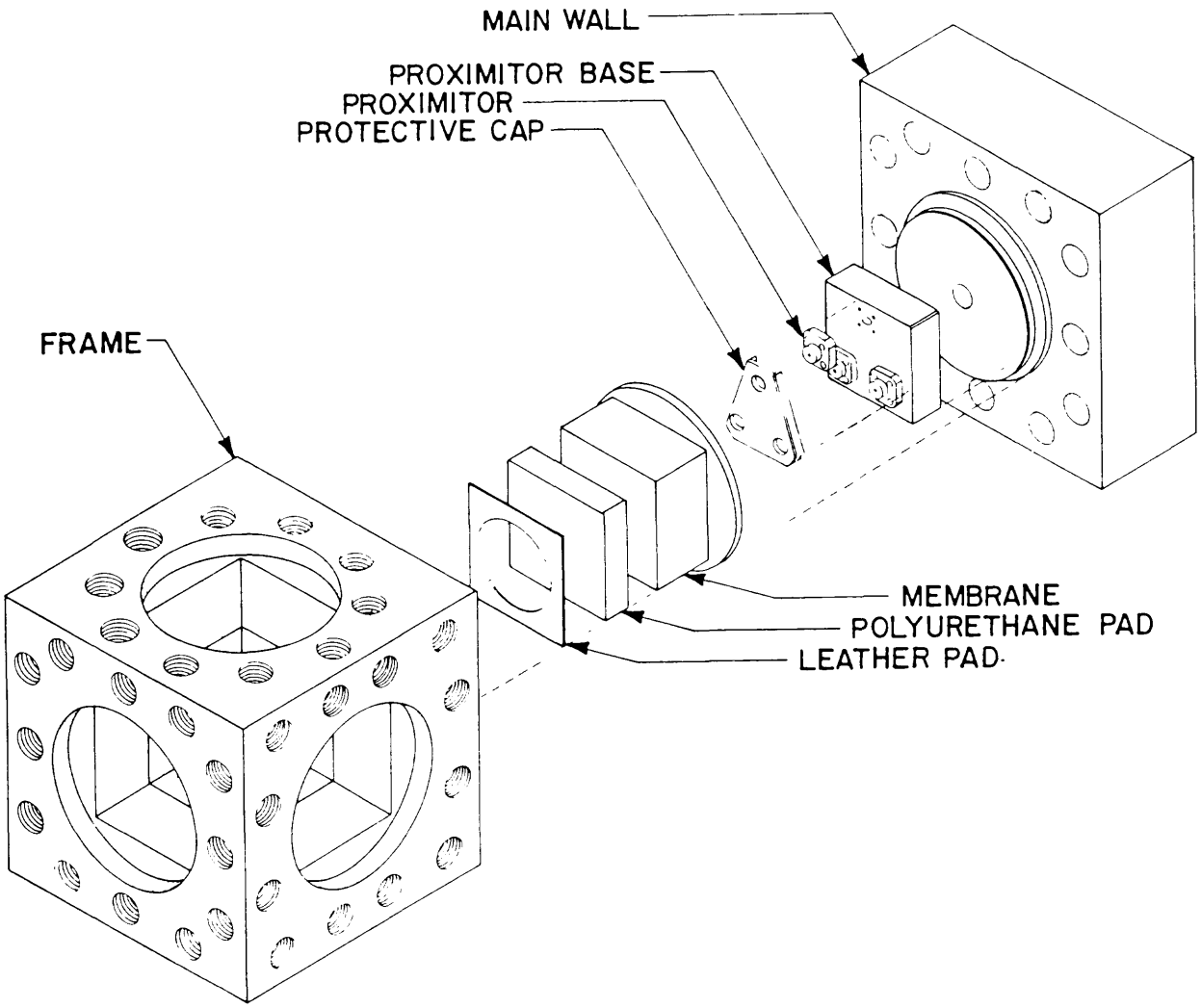

Figure 1. Expanded view of the multiaxial testing apparatus, the compression loading systems and other components. (Modified after Desai and others, 1982).

Experimental Results

The cube of Pierre Shale was tested in the multiaxial device at two confining pressures of 6.9 and 10.3 MPa (1,000 and 1,500 psi). The cube of shale was oriented in the testing device such that bedding was horizontal in the x-y plane and perpendicular to the vertical z-direction. In the first sequence of tests, the sample was initially subjected to a hydrostatic confining pressure of 6.9 MPa. This served as the reference pressure for subsequent deformation experiments along three principal stress directions. From this reference pressure, the pressure in the x-direction, parallel to bedding, was increased in steps of 0.34 MPa (50 psi) to a maximum of 9.0 MPa (1,300 psi) and then decreased in similar steps, while the pressure in the other two directions (y and z) were maintained at the reference level. Complete stress and displacement data were obtained at each step. Separate loading in the y- and z-directions was carried out in the same manner. The entire testing procedure was repeated at the higher confining pressure of 10.3 MPa (1,500 psi) and sequential loading tests were conducted in each direction to 12.4 MPa (1,800 psi).

The test results are summarized in Table 1. A slight dependence of the Young's moduli on confining pressure is apparent. Otherwise, the data sets obtained at two confining pressures are consistent and reproducible. Note the two high values for ν_{xz} and ν_{yz} characterizing the strain response perpendicular to bedding to loading in the bedding plane. These values are acceptable because elastic orthotropic materials have ranges of Poisson's ratios ν_{xz} and ν_{yz} given by:

$$-\sqrt{\frac{E_x}{E_z}} < \nu_{xz} < \sqrt{\frac{E_x}{E_z}} \qquad \text{and} \qquad -\sqrt{\frac{E_y}{E_z}} < \nu_{yz} < \sqrt{\frac{E_y}{E_z}}$$

These ranges are based on thermodynamic considerations of strain energy and symmetry requirements (Amadei and others, 1987).

TABLE 1. Deformation Properties of Pierre Shale.
[Leaders (---) indicate no data]

Applied Stress (MPa)			Young's Modulus (GPa)			Poisson's Ratio*					
σ_x	σ_y	σ_z	E_x	E_y	E_z	ν_{xy}	ν_{xz}	ν_{yx}	ν_{yz}	ν_{zx}	ν_{zy}
9.0	6.9	6.9	0.63	---	---	0.33	0.83	---	---	---	---
6.9	9.0	6.9	---	0.45	---	---	---	0.20	1.15	---	---
6.9	6.9	9.0	---	---	0.19	---	---	---	---	0.34	0.31
12.4	10.3	10.3	0.65	---	---	0.33	0.80	---	---	---	---
10.3	12.4	10.3	---	0.50	---	---	---	0.21	1.11	---	---
10.3	10.3	12.4	---	---	0.24	---	---	---	---	0.40	0.31

* ν_{ij} denotes the strain in the j direction due to stress in the i direction.

DISCUSSION

Constitutive Relations

The elastic behavior of Pierre Shale can be characterized by a compliance matrix relating strains to stresses. For an orthotropic material, this relation is:

$$\begin{bmatrix} \varepsilon_x \\ \varepsilon_y \\ \varepsilon_z \\ \gamma_{yz} \\ \gamma_{xz} \\ \gamma_{xy} \end{bmatrix} = \begin{bmatrix} \frac{1}{E_x} & \frac{-\nu_{yx}}{E_y} & \frac{-\nu_{zx}}{E_z} & 0 & 0 & 0 \\ \frac{-\nu_{xy}}{E_x} & \frac{1}{E_y} & \frac{-\nu_{zy}}{E_z} & 0 & 0 & 0 \\ \frac{-\nu_{xz}}{E_x} & \frac{-\nu_{yz}}{E_y} & \frac{1}{E_z} & 0 & 0 & 0 \\ 0 & 0 & 0 & \frac{1}{G_{yz}} & 0 & 0 \\ 0 & 0 & 0 & 0 & \frac{1}{G_{xz}} & 0 \\ 0 & 0 & 0 & 0 & 0 & \frac{1}{G_{xy}} \end{bmatrix} \cdot \begin{bmatrix} \sigma_x \\ \sigma_y \\ \sigma_z \\ \tau_{yz} \\ \tau_{xz} \\ \tau_{xy} \end{bmatrix}$$

where E_i are the Young's moduli, ν_{ij} the Poisson's ratios, and G_{ij} the shear moduli. The notation for the shear compliance $1/G_{yz}$ means, for example, the shear strain response γ_{yz} to the shear stress τ_{yz}. Similarly, the Poisson's ratio ν_{yx} characterizes the extensile strain response in the x-direction to a compressive stress in the y-direction.

The experimental results listed in Table 1 may be used to compute the numerical values of the diagonal and off-diagonal terms in the upper lefthand quadrant of the compliance matrix. Determination of the shear moduli G_{yz}, G_{xz}, and G_{xy} requires additional tests on three separate cubes of shale, each of which is rotated 45° about each of the material axes (Ko and Gerstle, 1976). Thus, to determine the shear modulus G_{yz} a new cube should be prepared with the y- and z- axes of the material rotated 45° about the x-axis in the bedding plane. None of these additional cubes of shale were available for testing in this feasibility study.

State of Stress

Consider the stress field induced in anisotropic Pierre Shale under the effect of gravity and vanishing horizontal displacements (Amadei and others, 1987). The crustal environment envisioned here is a tectonically quiescent setting in which the rock mass is homogeneous, linearly elastic and orthotropic. The constitutive model of the shale is described by the stress-strain relation given in the previous section. If the lateral strains vanish, that is $\varepsilon_x = \varepsilon_y = 0$, and the vertical stress component $\sigma_z = \rho gh$, the stress-strain relation reduces to the two equations for the two unknowns σ_x and σ_y,

$$\varepsilon_x = 0 = \frac{\sigma_x}{E_x} - \frac{\nu_{yx}}{E_y}\sigma_y - \frac{\nu_{zx}}{E_z}\rho gh$$

$$\varepsilon_y = 0 = \frac{\sigma_y}{E_y} - \frac{\nu_{xy}}{E_x}\sigma_x - \frac{\nu_{zy}}{E_z}\rho gh$$

or equivalently,

$$\frac{\sigma_x}{E_x} - \frac{\nu_{yx}}{E_y}\sigma_y = \frac{\nu_{zx}}{E_z}\rho gh$$

$$\frac{\sigma_y}{E_y} - \frac{\nu_{xy}}{E_x}\sigma_x = \frac{\nu_{zy}}{E_z}\rho gh$$

By inversion and by using the symmetry conditions,

$$\frac{\nu_{xy}}{E_x} = \frac{\nu_{yx}}{E_y} \quad ; \quad \frac{\nu_{xz}}{E_x} = \frac{\nu_{zx}}{E_z} \quad ; \quad \frac{\nu_{yz}}{E_y} = \frac{\nu_{zy}}{E_z}$$

the equations for the horizontal stress σ_x and σ_y may now be written as (Amadei and others, 1987):

$$\sigma_x = \frac{(\nu_{xz} + \nu_{yz}\nu_{xy})}{1 - \nu_{xy}\nu_{yx}}\rho gh$$

$$\sigma_y = \frac{(\nu_{yz} + \nu_{yx}\nu_{xz})}{1 - \nu_{xy}\nu_{yx}}\rho gh$$

Note that these equations for σ_x and σ_y are independent of E_x, E_y, and E_z.

At a depth of $h = 700$ m, the vertical stress in Pierre Shale of density $\rho = 2.16$ gm/cm^3 is equal to $\sigma_z = \rho gh = 14.8$ MPa. Using the elastic property values in Table 1, it follows that σ_x can range from 18.5 to 19.2 MPa and σ_y can range from 20.3 to 20.9 MPa.

The magnitudes of both horizontal stresses depend on the degree of anisotropy of the rock and, in the present case, exceed the vertical stress component. The resultant gravity-induced stress field in thinly bedded shale is multiaxial. This result contrasts sharply with the case of an isotropic medium, where the horizontal stress components could not exceed the vertical stress, unless the rock mass is subjected to a tectonic compression of regional extent.

CONCLUSIONS

A 10-cm cube of Pierre Shale has been tested under confining pressure and incremental compressive loads along three principal material directions. The results of these deformation experiments show that the shale behaves as an orthotropic material. The properties measured in a direction perpendicular to bedding (e.g., E_z, ν_{xz}, and ν_{yz}) deviate significantly from those measured in the plane of bedding. Using these measured properties and the constitutive behavior of Pierre Shale, it can be shown that the stress field, developed in place at shallow crustal depths, is itself anisotropic. In the absence of regional tectonic considerations, the gravity-induced stress field is multiaxial and the magnitudes of the horizontal stress components exceed that of the vertical component of stress due to the weight of overburden.

REFERENCES

Akai, K., Yamamoto, K., and Arioka, M., 1970, Experimental research on the structural anisotropy of crystalline schists, in Proceedings, 2d International Congress of the International Society for Rock Mechanics, Belgrade, v. 2, 3-26, p. 181-186 (in German).

Amadei, B., Savage, W.Z., and Swolfs, H.S., 1987, Gravitational stresses in anisotropic rock masses: International Journal of Rock Mechanics and Mining Sciences & Geomechanics Abstracts, v. 24, no. 1, p. 5-14.

Desai, C.S., Janardahanam, R., and Sture, S., 1982, High capacity multiaxial testing device: Geotechnical Testing Journal, v. 5, no. 1/2, p. 26-33.

Ko, H.Y., and Gerstle, K.H., 1976, Elastic properties of two coals: International Journal of Rock Mechanics and Mining Sciences & Geomechanics Abstracts, v. 13, no. 3, p. 81-90.

Mogi, K., 1971, Fracture and flow of rocks under high triaxial compression: Journal of Geophysical Research, v. 76, no. 5, p. 1255-1269.

Reches, Z., and Dieterich, J.H., 1983, Faulting of rocks in three-dimensional strain fields-1--Failure of rocks in polyaxial, servo-control experiments: Tectonophysics, v. 95, p. 111-132.

Reik, G., and Zacas, M., 1978, Strength and deformation characteristics of jointed media in true triaxial compression: International Journal of Rock Mechanics and Mining Sciences & Geomechanics Abstracts, v. 15, no. 6, p. 295-303.

Swolfs, H.S., 1984, The triangular stress diagram--a graphical representation of crustal stress measurements: U.S. Geological Survey Professional Paper 1291, p. 19.